LBL-18253
c.2

Lawrence Berkeley Laboratory
UNIVERSITY OF CALIFORNIA

RECEIVED
LAWRENCE
BERKELEY LABORATORY
OCT 9 1984
LIBRARY AND
DOCUMENTS SECTION

Materials & Molecular Research Division

Presented in part at the 16th Rare Earth Research Conference, Tallahasse, FL, April 18-21, 1983; and submitted to Spectrochimica Acta

THE ELECTRONIC STRUCTURE OF ORGANOMETALLIC COMPLEXES OF THE f ELEMENTS XI. ABSORPTION SPECTRUM AND PARAMETERIZATION OF THE CRYSTAL FIELD SPLITTING PATTERN OF A METHYLTETRAHYDROFURAN ADDUCT DERIVED FROM TRIS(η^5-CYCLOPENTADIENYL)-PRASEODYMIUM(III)

H.-D. Amberger, H. Schultze, and N.M. Edelstein

August 1984

TWO-WEEK LOAN COPY
This is a Library Circulating Copy which may be borrowed for two weeks

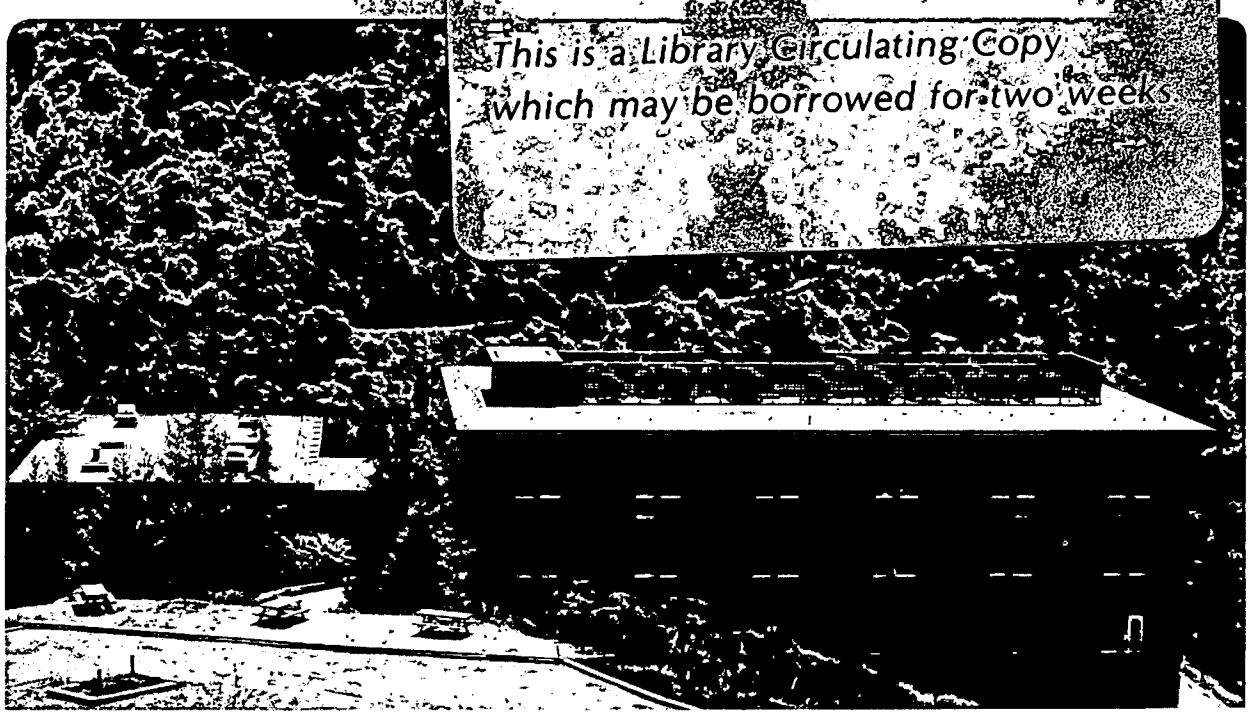

LBL-18253
c.2

Prepared for the U.S. Department of Energy under Contract DE-AC03-76SF00098

DISCLAIMER

This document was prepared as an account of work sponsored by the United States Government. While this document is believed to contain correct information, neither the United States Government nor any agency thereof, nor the Regents of the University of California, nor any of their employees, makes any warranty, express or implied, or assumes any legal responsibility for the accuracy, completeness, or usefulness of any information, apparatus, product, or process disclosed, or represents that its use would not infringe privately owned rights. Reference herein to any specific commercial product, process, or service by its trade name, trademark, manufacturer, or otherwise, does not necessarily constitute or imply its endorsement, recommendation, or favoring by the United States Government or any agency thereof, or the Regents of the University of California. The views and opinions of authors expressed herein do not necessarily state or reflect those of the United States Government or any agency thereof or the Regents of the University of California.

LBL-18253

The Electronic Structure of Organometallic Complexes of the f Elements XI. Absorption Spectrum and Parameterization of the Crystal Field Splitting Pattern of a Methyltetrahydrofuran Adduct Derived from Tris(η^5-cyclopentadienyl)-praseodymium(III)*

H.-D. Amberger and H. Schultze
Institut fur Anorganische und Angewandte Chemie der Universitat Hamburg
Martin-Luther-King-Platz 6
D-2000 Hamburg 13, F.R. Germany

N.M. Edelstein
Materials and Molecular Research Division
Lawrence Berkeley Laboratory
University of California
Berkeley, California 94720

Abstract

The low temperature absorption spectrum of tris(η^5-cyclopentadienyl)-praseodymium(III) dissolved in a 2-methyltetrahydrofuran glass has been measured. The observed transitions, along with the previously reported magnetic circular dichroism transitions, have been assigned and fit to the parameters of a semiempirical Hamiltonian with an rms deviation of 27.2 cm^{-1} for 40 levels. The experimental and calculated magnetic susceptibility of Cp_3Pr•butyl acetate (which has an optical spectrum very similar to that of Cp_3Pr•MeTHF) as a function of temperature are also given.

---

*Reported in part at the 16th Rare Earth Research Conference, Tallahassee, Florida, U.S.A., April 18-21, 1983.

1. Introduction

In the late sixties and early seventies considerable effort was expended to elucidate the electronic structures of adducts of tris(η^5-cyclopentadienyl)-lanthanide(III) complexes (= Cp_3Ln add) on the basis of absorption, [1-8] magnetochemical, [9,10] and NMR spectroscopic [11,12] measurements. Little progress was made during this period so the problem was set aside. Subsequently, some detailed studies on the molecular and crystal structure of $Cp_3Pr{\cdot}CNC_6H_{11}$ [13] and $Cp_3La{\cdot}THF$ [14] were reported. According to these investigations the lanthanide ion is surrounded by the centroids of the three Cp rings and the complexing atom of the base in the shape of a somewhat distorted trigonal pyramid. Therefore, the effective crystal field (= CF) is of nearly C_{3v} symmetry.

In 1983 Brittain et al. studied the luminescence of the transitions $^5D_4 \rightarrow {}^7F_J$ (J = 0 - 6) of $Cp_3Tb{\cdot}THF$ and $(MeCp)_3Tb{\cdot}THF$ [15]. With the exception of the transition $^5D_4 \rightarrow {}^7F_0$ the number of the observed bands was less than the expected number. For this reason only the truncated CF splitting pattern of the manifold $^5D_4$ could be determined, but no assignments were made [15].

Recently Amberger et al. assigned 17 signals in the low temperature MCD spectrum of $Cp_3Pr{\cdot}MeTHF$ and $Cp_3Pr{\cdot}CNC_6H_{11}$, respectively [16]. On the basis of these assignments preliminary sets of Slater, spin orbit and CF parameters were derived for these molecules [16].

In this paper the observed bands in the low temperature

absorption spectrum of $Cp_3Pr \cdot MeTHF$ are assigned by comparing the energies of the observed transitions with the previously calculated energies. From these assignments a new set of parameters has been obtained by a least-squares fitting procedure.

2. Experimental

The preparation of the compounds and the experimental details have been described previously [16-18]. At the time that the optical data reported in this paper were analyzed, no sample of $Cp_3Pr \cdot MeTHF$ was available so as to obtain magnetic susceptibility data. It has been noted that the optical spectrum of $Cp_3Pr \cdot$butylacetate ($Cp_3Pr \cdot BA$) is very similar to that of $Cp_3Pr \cdot MeTHF$ [19]. Therefore the ester complex was used for magnetic measurements. The apparatus used has been described previously [20].

3. Assignment of the Observed Bands of the Low Temperature Absorption Spectrum

Previous optical and magnetochemical investigations showed that $Cp_3Pr \cdot$add complexes have an A_1 ground state [16-18]. As the first excited state is separated by ~100 cm^{-1}, the use of liquid He as cooling agent (the actual temperature of the sample is about 15-30 K) allows only the ground CF state to be appreciably thermally populated. According to the selection rules for forced electric dipole radiation for strictly C_{3v} symmetry, transitions to excited A_1 and E levels are allowed, whereas transitions to A_2 levels are

forbidden. Because of a small distortion from the ideal C_{3v} symmetry of the effective CF [13-18], weak transitions to A_2 levels may be observed. Additional weak bands are produced by vibronic coupling effects. In the far infrared spectrum of $Cp_3Pr \cdot add$ distinct signals were observed at 70-80, 130-150, 220-240, and 410-440 cm^{-1}. Weak signals on the blue side of strong bands which have energy separations of these values (or linear combinations of them) may be of vibronic origin. Further bands in the region 3900-4570 cm^{-1} and a band at 6100 cm^{-1} are due to a combination of vibrations [21].

$^3H_4$

A comparison of the room temperature absorption spectrum with the liquid He spectrum showed that many intense bands are accompanied on their red side by additional bands with energy separations of 97, 310 and 756 cm^{-1}, respectively. By means of magnetooptical measurements, the hot bands of the transition $^3H_4 \rightarrow {}^3P_0$ could be identified with $1E(^3H_4) \rightarrow 14A_1(^3P_0)$, $2E(^3H_4) \rightarrow 14A_1(^3P_0)$ and $3E(^3H_4) \rightarrow 14A_1(^3P_0)$ [18].

No attempts were made to observe the transition $^3H_4 \rightarrow {}^3H_5$.

$^3H_6$ (Figures 1,2)

It is difficult to observe the transition $^3H_4 \rightarrow {}^3H_6$ in solution, as combination bands of the common organic solvents appear in this region. For this reason the absorption spectrum was run in a

KBr pellet. The use of either liquid N_2 or liquid He as a cooling agent did not change the spectra substantially. The actual temperature of the sample was probably in the range 80-100 K. Besides the cold transitions 0-3 some hot bands and some vibrational combination bands could be observed. The signals of vibrational origin could be identified by comparison with the corresponding bands of $ScCp_3$ and $NdCp_3$, respectively [21]. Bands 0-5 are in immediate neighborhood of the corresponding calculated energies so that they were easily identified.

$^3F_2$ (Figure 2)

As bands 6, 7 and 8 match the corresponding calculated energies very well they can be assigned without any doubt. At cryogenic temperatures there is an additional signal which appears between bands 6 and 7 and is separated by 127 cm^{-1} from band 6. As a signal with a comparable energy appears in the FIR spectrum, the above band is presumably due to vibronic coupling effects.

$^3F_3$ (Figure 2)

The weak signal 9 is due to the forbidden transition $1A_1(^3H_4) \rightarrow 6A_2(^3F_3)$. Because of the selection rules the allowed hot transition $1E(^3H_4) \rightarrow 6A_2(^3F_3)$ is much more intense even at liquid N_2 temperatures. As the sample seems to heat up somewhat in the NIR radiation this hot band is observable even if liquid He is used as a cooling agent. Bands 10, 11 and 12, respectively, match the

calculated energies very well, but the assignment of the weak signal 11 is somewhat doubtful. It could also correspond to a vibronic (ΔE = 124 cm^{-1} from band 10) or to a hot transition (ΔE = 85 cm^{-1} from band 12. In order to determine its origin we inspected the corresponding spectral region of $Cp_3Pr{\cdot}CNC_6H_{11}$ where the above mentioned coincidences do not take place. As there was a comparable intensity pattern of bands 10, 11 and 12 of $Cp_3Pr{\cdot}CNC_6H_{11}$ we assign signal 11 to the purely electronic transition $1A_1(^3H_4) \rightarrow 15E(^3F_3)$.

$^3F_4$ (Figure 2)

The transition $^3H_4 \rightarrow {}^3F_4$ corresponds only to three signals, the sharp band 13, the relative broad intense curve 14 and a poorly resolved signal (with some shoulders) with a maximum at 1370 nm. In the same spectral region $Cp_3Pr{\cdot}CNC_6H_{11}$ exhibits five sharp bands [17]. This suggests that some accidental degeneracies might take place. Comparing both absorption spectra with the corresponding calculated CF energies we make the following tentative assignments: signal 13 corresponds simultaneously to the transitions $1A_1(^3H_4) \rightarrow 9A_1(^3F_4)$ and $16E(^3H_4)$ and band 14 to the transitions $1A_1(^3H_4) \rightarrow 17E(^3F_4)$ and $18E(^3F_4)$. The weak shoulders at 7246 and 7273 cm^{-1} of the curve on the blue side of band 14 can also be tentatively explained: either they are due to the transitions $1A_1(^3H_4) \rightarrow 10A_1(^3F_4)$ and $1A_1(^3H_4) \rightarrow 8A_2(^3H_4)$ (calculated at 7221 and 7275 cm^{-1}) or they are due to vibronic coupling effects (7012 + 230 = 7242; 7153 + 130 =

7283 cm^{-1}).

$^1G_4$ (Figure 3)

The spin forbidden transitions $^3H_4 \rightarrow {}^1G_4$ have extremely low molar extinction coefficients. Even in saturated solutions no distinct bands could be observed. However the solubility of $(MeCp)_3Pr \cdot MeTHF$ in MeTHF is considerably enhanced so that this transition can be observed. For this reason we studied this transition with $(MeCp)_3Pr \cdot MeTHF$. At room temperature the absorption spectra of $Cp_3Pr \cdot add$ and $(MeCp)_3Pr \cdot add$ are nearly identical [19], but at low temperatures some transitions to degenerate excited levels are split. According to the selection rules of C_{3v} symmetry five bands are expected at liquid He temperatures. As only a liquid N_2 spectrum was obtained, the first excited CF level is also appreciably thermally populated, so that some additional hot bands (ΔE = 97 cm^{-1}) appeared.

Band 19 is split into two components with an energy separation of 43 cm^{-1}. This indicates that it is due to a transition to an excited doublet. The only calculated doublet in this energy region is $21E(^1G_4)$ so that we assign band 19 to the transition $1A_1(^3H_4) \rightarrow 21E(^1G_4)$. The corresponding hot band also exhibits a splitting of some 40 cm^{-1}. Band 15 is also split into two components with an energy separation of 37 cm^{-1}. Using the same arguments as above we identify band 15 with the transition $1A_1(^3H_4) \rightarrow 19E(^1G_4)$. Assuming that the order of the calculated CF levels is correct the remaining three allowed transitions have to be assigned to bands 16,

17 and 18, respectively.

$^1D_2$ (Figure 4)

Bands 20, 21 and 22 have been previously identified on the basis of MCD measurements [16,18]. The correlation is indicated in Table 1. An additional weak signal at 589.1 nm is separated by 129 cm^{-1} from band 22 and is therefore presumably of vibronic origin.

$^3P_0$ (Figure 5)

The absorption and MCD transitions $^3H_4 \rightarrow {}^3P_0$ have been reported elsewhere [16,18]. The first two signals at the blue side of band 23 (with energy separations of 130 and 229 cm^{-1}) are due to vibronic coupling effects.

$^3P_1$ (Figure 5)

Three signals are observed at liquid He temperature between band 23 and bands 25, 26, but at liquid N_2 temperature four signals are found. The additional relatively intense hot band has an energy separation of 97 cm^{-1} from the very weak signal 24. These observations can be rationalized by identifying band 24 with the forbidden transition $1A_1(^3H_4) \rightarrow 10A_2(^3P_1)$ and the corresponding hot band with the allowed transition $2E(^3H_4) \rightarrow 10A_2(^3P_1)$. The overlapping bands 25 and 26 correspond to a superposition of a Faraday B (25) and a Faraday A term (26) in the MCD spectrum. Therefore signal 25 has to be assigned to the transition $1A_1(^3H_4) \rightarrow$

$15A_1(^1I_6)$ and band 26 to the transition $1A_1(^3H_4) \rightarrow 24E(^3P_1)$.

$^1I_6$ (Figure 5)

Bands 28, 30 and 35, respectively, have been assigned previously on the basis of the low temperature MCD spectrum, and the energies of the bands 25, 27 and 31 agree quite well with the corresponding calculated energies. The nature of band 29 is uncertain; either it has to be identified with the transition $1A_1(^3H_4) \rightarrow 16A_1(^1I_6)$ or it is due to a vibronic band ($\Delta E = 224\ cm^{-1}$ from band 27). On the blue side of band 30 is a weak signal ($\Delta E = 122\ cm^{-1}$ from band 30) which is presumably due to vibronic coupling effects.

$^3P_2$, $^1I_6$ (Figure 5)

Bands 32, 33, and 34 are in reasonable agreement with the calculated transition energies $1A_1(^3H_4) \rightarrow 29E(^3P_2)$, $1A_1(^3H_4) \rightarrow 17A_1(^3P_2)$ and $^1A_1(^3H_4) \rightarrow 30E(^3P_2)$, respectively, and are so assigned. A first order CF calculation shows bands 33-35 should be correlated with the transition $^3H_4 \rightarrow {}^3P_2$, but due to strong mixing via the CF, the CF eigenvector of $18A_1$ is dominated by $^1I_6$ and not by $^3P_2$; likewise $17A_1$ is dominated by $^3P_2$ instead of $^1I_6$.

$^1S_0$

The transition $^3H_4 \rightarrow {}^1S_0$ is obscured by strong charge

transfer bands.

4. Optical Analysis

The energy levels within f^n configuration in C_{3v} symmetry can be written in terms of the atomic free ion (H_{FI}) and crystal field (H_{CF}) Hamiltonians as follows: [22,23]

$$H = H_{FI} + H_{CF}$$

where

$$H_{FI} = \sum_{k=0,2,4,6} f_k F^k(nf,nf) + \zeta_f a_{so} + \alpha L(L+1)$$

$$+ \beta G(G_2) + \gamma(R_7) + \sum_{k=0,2,4} m_k M^k + \sum_{k=2,4,6} P_k P^k$$

and

$$H_{CF} = B_0^2 C_0^{(2)} + B_0^4 C_0^{(4)} + B_3^4(C_{-3}^{(4)} - C_3^{(4)})$$

$$+ B_0^6 C_0^{(6)} + B_3^6(C_{-3}^{(6)} - C_3^{(6)}) + B_6^6(C_{-6}^{(6)} + C_6^{(6)})$$

The $F^k(nf,nf)$'s and ζ_f represent, respectively, the radial parts of the electrostatic and spin-orbit interactions between f electrons, while f_k and a_{so} are the angular parts of the interactions. α, β, and γ are the parameters associated with the two-body effective operators of configuration interaction. The M^k parameters represent

the spin-spin and spin-other-orbit interactions while the P^k parameters arise from electrostatic-spin-orbit interactions with higher configurations. The crystal field interaction for C_{3v} symmetry is represented by the six B_q^k parameters and the tensor operators $C_q^{(k)}$ [23].

The assignments discussed previously were fit to the parameters of the above Hamiltonian by a least-squares routine. In order to limit the number of free parameters, γ, the M^k parameters, and the P^k parameters were fixed at the values used for the analysis of Pr^{3+}:$LaCl_3$ [24]. The remaining parameters were allowed to vary. For 40 levels the rms deviation was 27.2 cm^{-1}. A comparison of the experimental and calculated energies is shown in Table 1 while Table 2 gives the final values of the free ion and crystal field parameters. For comparison purposes, parameters for the Pr^{3+} free ion [25] and Pr^{3+}:$LaCl_3$ [24] are also listed.

Magnetic Susceptibility Results

Magnetic data for the compound $Cp_3Pr{\cdot}BA$ are shown in Figure 6. Because of the similarities of the optical spectra of $Cp_3Pr{\cdot}MeTHF$ and $Cp_3Pr{\cdot}BA$, we have assumed the wavefunctions obtained from the optical analysis of $Cp_3Pr{\cdot}MeTHF$ can be used to calculate the magnetic susceptibility of $Cp_3Pr{\cdot}BA$. The magnetic susceptibility measured in the 2-300 K temperature range depends primarily on the crystal field splittings of the lowest J manifold. The calculated energies of the lowest two E states have been replaced by the actual

experimental energies in the magnetic susceptibility calculation. These energies are shown in Table 3. The calculated susceptibilities are also shown in Figure 6.

Three different values of the orbital reduction constant k (as defined in the modified Zeeman Hamiltonian $\langle\psi|k\vec{L} + 2\vec{S}|\psi\rangle$ are shown in Figure 6: the upper curve is for k = 0.95, the middle curve for k = 0.975, and the lower curve for k = 1.00. Clearly the curve with k = 0.975 fits the experimental data most satisfactorily.

Discussion

This work represents the first complete optical analysis of an organometallic f element compound. Some of the earlier studies have resulted in estimates of the second order crystal field parameter B_0^2 based on absorption or proton magnetic resonance spectroscopic measurements. Hayes and Thomas [26] estimated values for B_0^2 of 2420 cm^{-1} and 1368 cm^{-1} for $Cp_3Nd{\cdot}MeTHF$ and $Cp_3Er{\cdot}MeTHF$, respectively, from the splittings of excited J = 3/2 states and the application of first order crystal field theory. They also calculated a value for B_0^2 of ~ -528 cm^{-1} using an electrostatic model and assuming C_{3h} symmetry for the hypothetical free $M(C_5H_5)_3$ molecule ($M = Ln^{3+}$).

This calculated negative sign was supported by the NMR investigations of Fischer and Amberger [11] and Jahn et al. [27] who analyzed the observed isotropic NMR shifts of the δ cyclohexyl protons (where the contact contribution can be neglected) of $Cp_3Ln{\cdot}CNC_6H_{11}$ (Ln = Pr,

Nd) on the basis of Bleaney's formula for the dipolar contribution [28].

The only previous attempt to estimate values for B_0^2, B_0^4, and B_0^6 (neglecting B_3^4, B_3^6 and B_6^6) for $Cp_3Ln{\cdot}L$ compounds was due to Aderhold [29]. By fitting the temperature dependence of the paramagnetic susceptibility of $Cp_3Yb{\cdot}CNC_6H_{11}$ within the range 4.2-302 K, he found B_0^2 = -563, B_0^4 = 614 and B_0^6 = 5250 cm^{-1}. The signs of these parameters agree with the corresponding ones of Table 2. His values of B_0^2 and B_0^4 are of the correct order of magnitude, but B_0^6 is off a factor of 7 (presumably because of neglecting the substantial contribution of B_6^6). However only qualitative agreement could be expected for a comparison of the crystal field paramters $Cp_3Pr{\cdot}L$ and $Cp_3Yb{\cdot}L$.

Auzel and Malta [30] have defined the parameter

$$\frac{Nv}{\sqrt{4\pi}} = [\sum_{k,q} \frac{1}{2k+1} (B_q^k)^2]^{1/2}$$

which is a measure of the relative strengths of the crystal field of ions in various site symmetries. From the parameters listed in Table 2, $Nv/\sqrt{4\pi}$ is equal to 259 cm^{-1} for $Pr^{3+}/LaCl_3$ and 936 cm^{-1} for $Cp_3Pr{\cdot}MeTHF$. Thus using this criterion, the crystal field for $Cp_3Pr{\cdot}MeTHF$ is approximately three times greater than for $Pr^{3+}/LaCl_3$.

The values of the Slater parameters and the spin-orbit coupling constant for transition metal ions in crystals and molecules are smaller than the values found in the free ion. The extent of this reduction has been used as a measure of the covalency of the complex [31]. Newman has suggested that the reduction in the values of the

Slater parameters should be correlated with the ligand polarizability [32], but calculations by other workers have shown (for d transition metal ions and U^{4+}) [33,34] that this mechanism does not account for the large reductions found empirically. Some values of various ratios for Pr^{3+} and U^{4+} ($4f^2$ and $5f^2$) are shown in Table 4.

From Table 4 one immediately can note the similarity between the ratios for $Pr^{3+}/LaCl_3$ and $Cp_3Pr{\cdot}MeTHF$ and the differences with the ratios for $U^{4+}/ThBr_4$ and $U(BD_4)_4$. Clearly F^2 is much more affected by the crystalline environment than F^4 or F^6 so that in cases where free ion data is not available the ratio F^4/F^2 could be used to compare the same ion in different environments. The reduction found for the spin-orbit coupling constant in $Cp_3Pr{\cdot}MeTHF$ agrees very well with the value of the orbital reduction constant ($k = 0.975$) found from the magnetic measurements. Thus, even though the crystal field is ~ 3 times larger in $Cp_3Pr{\cdot}MeTHF$ than in $Pr^{3+}/LaCl_3$, the reduction in F^2 and ζ is the same for these two compounds.

Acknowledgements

One of us (H.-D.A.) would like to thank the Deutsche Forschungsgemeinschaft for financial support of his research scholarship at the Lawrence Berkeley Laboratory, and the Fonds der Chemischen Industrie for financial support. We thank Dr. K. Rajnak for valuable discussisons.

This work was supported by the Director, Office of Energy

Research, Office of Basic Energy Sciences, Chemical Sciences Division of the U.S. Department of Energy under Contract No. DE-AC03-76SF00098.

References

[1] R. Pappalardo, Helv. Phys. Acta 38, 179 (1965).

[2] R.D. Fischer and H. Fischer, J. Organomet. Chem. 4, 412 (1965).

[3] R. Pappalardo, 5th Rare Earth Research Conference, Ames (Iowa), USA, August 1965.

[4] F. Calderazzo, R. Pappalardo and S. Losi, J. Inorg. Nucl. Chem. 28, 987 (1966).

[5] R. Pappalardo and C.K. Jorgensen, J. Chem. Phys. 46, 632 (1967).

[6] R.D. Fischer and H. Fischer, J. Organomet. Chem. 8, 155 (1967).

[7] R. Pappalardo, J. Chem. Phys. 49, 1545 (1968).

[8] R. Pappalardo, J. Molec. Spectry. 29, 13 (1969).

[9] B. Kanellakopulos and C. Aderhold, XXIV. IUPAC Conference, Hamburg, FRG, September 2-8, 1973.

[10] B. Kanellakopulos, unpublished results.

[11] R.D. Fischer and H.-D. Amberger, 10th Rare Earth Research Conference, Carefree (Arizona), USA, April 30-May 3, 1973, page 15.

[12] H. Wagner, Thesis, Heidelberg, 1974.

[13] J.H. Burns and W.H. Baldwin, J. Organomet. Chem. 120, 361 (1976).

[14] R.D. Rogers, J.L. Atwood, E. Emad, D.J. Sikora and M.D. Rausch, J. Organomet. Chem. 216, 383 (1981).

[15] H.G. Brittain, J.H. Meadows and W.J. Evans, Organometallics 2, 1661 (1983).

[16] H.-D. Amberger, W. Jahn and N.M. Edelstein, submitted to Spectrochimica Acta A.

[17] H.-D. Amberger and W. Jahn, submitted to Spectrochimica Acta A.

[18] H.-D. Amberger and W. Jahn, submitted to Spectrochim. Acta.

[19] H.-D. Amberger, unpublished results, 1983.

[20] K. Rajnak, E. Gamp, R. Shinomoto, and N. Edelstein, J. Chem. Phys. 80, 5942 (1984).

[21] A.F. Reid, D.E. Scaife and P.C. Wailes, Spectrochim. Acta 20, 1257 (1964).

[22] W.T. Carnall, H. Crosswhite, H.M. Crosswhite, J.P. Hessler, N.M. Edelstein, J.G. Conway, G.V. Shalimoff, and R. Sarup, J. Chem. Phys. 72, 5089 (1980).

[23] B.G. Wybourne, "Spectroscopic Properties of Rare Earths," (Wiley, New York, 1965).

[24] W.T. Carnall, H. Crosswhite, and H.M. Crosswhite, "Energy Level Structure and Transition Probabilities in the Spectra of the Trivalent Lanthanides in LaF_3," Argonne National Laboratory, 1977, unpublished.

[25] H.M. Crosswhite and H. Crosswhite, J. Opt. Soc. Am. B 1, 246 (1984).

[26] R.G. Hayes and J.L. Thomas, Organomet. Chem. Rev. A7, 1 (1971).

[27] W. Jahn, R. Yunlu, W. Oroschin, H.-D. Amberger and R.D. Fischer, Inorg. Chimica Acta, in print.

[28] B. Bleaney, J. Magnetic Resonance 8, 91 (1972).

[29] C. Aderhold, Thesis, Heidelberg, 1974.

[30] F. Auzel and O.L. Malta, J. Phys. (Paris) 44, 201 (1983).

[31] A.B.P. Lever, "Inorganic Electronic spectroscopy," (Elsevier, New York, 1968).

[32] D.J. Newman, Austr. J. Phys. 30, 315 (1977).

[33] M.V. Eremin and A.A. Kornienko, Opt. Spectrosc. (USSR) 53, 45 (1982).

[34] P. Delamoye, K. Rajnak, M. Genet, and N. Edelstein, Phys. Rev. B 28, 4923 (1983).

Table 1. Experimental and calculated energies of $(Cp_3)Pr{\cdot}MeTHF$

Band Number[a]	State	E_{calc} (cm^{-1})	E_{obs} (cm^{-1})	ΔE[b] (cm^{-1})	Eigenvector[c]
	$1A_1$	0.0	0.0		$96.8\ ^3H_4 + 2.6\ ^1G_4$
	1E	115.7	97.	18.7	$95.9\ ^3H_4 + 2.5\ ^1G_4 + 1.2\ ^3H_5$
	2E	315.5	310.	5.5	$94.2\ ^3H_4 + 2.9\ ^3H_5 + 2.6\ ^1G_4$
	$1A_2$	340.9			$95.9\ ^3H_4 + 2.0\ ^1G_4 + 1.8\ ^3H_5$
	3E	715.0	756.	-41.0	$92.8\ ^3H_4 + 3.5\ ^1G_4 + 1.7\ ^3H_5$
	$2A_1$	830.7			$92.4\ ^3H_4 + 3.5\ ^1G_4 + 2.5\ ^3H_5$
	$2A_2$	2159.4			$99.3\ ^3H_5$
	4E	2213.9			$95.8\ ^3H_5 + 1.8\ ^3H_4 + 1.7\ ^3H_6$
	5E	2355.5			$97.0\ ^3H_5 + 1.8\ ^3H_6$
	$3A_1$	2446.4			$94.0\ ^3H_5 + 2.5\ ^3H_4 + 2.2\ ^3H_6$
	6E	2691.9			$91.0\ ^3H_5 + 4.7\ ^3F_2 + 2.2\ ^3H_4$
	$3A_2$	2796.3			$95.9\ ^3H_5 + 1.6\ ^3H_4 + 1.25\ ^3H_6$
	7E	2801.9			$96.1\ ^3H_5 + 1.7\ ^3F_2 + 1.0\ ^3H_4$
0	$4A_1$	4192.0	4185.	7.0	$97.0\ ^3H_6$
	8E	4262.6			$96.8\ ^3H_6 + 1.1\ ^3F_3$
1	9E	4422.7	4434.	-11.3	$97.0\ ^3H_6 + 1.6\ ^3F_5$
	$4A_2$	4431.9			$96.7\ ^3H_6 + 1.9\ ^3F_3$
2	$5A_1$	4639.3	4651.	-11.7	$65.7\ ^3H_6 + 30.3\ ^3F_2 + 1.1\ ^3F_4$
3	10E	4809.7	4803.	6.7	$73.2\ ^3H_6 + 19.2\ ^3F_2 + 3.2\ ^3F_3 + 1.8\ ^3H_5 + 1.6\ ^3F_4$
	$5A_2$	4886.5			$90.9\ ^3H_6 + 7.6\ ^3F_3$
4	11E	4995.1	4980.	15.1	$78.9\ ^3H_6 + 12.6\ ^3F_2 + 3.6\ ^3F_3 + 2.5\ ^3F_4 + 1.4\ ^3H_5$
5	$6A_1$	5084.9	5076.	8.9	$87.9\ ^3H_6 + 4.7\ ^3F_2 + 3.3\ ^3F_4$
6	12E	5182.0	5189.	-7.0	$72.4\ ^3F_2 + 16.8\ ^3H_6 + 4.7\ ^3F_4 + 2.1\ ^3H_5 + 1.9\ ^1D_2 + 1.4\ ^1G_4$
7	13E	5431.7	5391.	40.7	$78.0\ ^3F_2 + 13.3\ ^3H_6 + 3.1\ ^3H_5 + 2.5\ ^3F_3 + 2.1\ ^1D_2$
8	$7A_1$	5533.6	5537.	-3.4	$61.2\ ^3F_2 + 33.6\ ^3H_6 + 2.8\ ^3F_4$
9	$6A_2$	6250.0	6289.	-39.0	$95.2\ ^3F_3 + 3.7\ ^3F_4$
10	14E	6591.7	6596.	-4.3	$92.1\ ^3F_3 + 3.4\ ^3F_4 + 1.9\ ^3H_6 + 1.1\ ^1G_4$

Table 1 continued.

Band Number[a]	State	E calc (cm^{-1})	E obs (cm^{-1})	ΔE[b] (cm^{-1})	Eigenvector[c]
11	15E	6730.7	6720.	10.7	80.3 $^3F_3$ + 11.1 $^3F_4$ + 3.6 $^1G_4$ + 3.2 $^3H_6$
12	$8A_1$	6806.9	6805.	1.9	91.3 $^3F_3$ + 3.8 $^3H_6$ + 2.0 $^3F_4$ + 1.0 $^1G_4$
	$7A_2$	6832.2			85.8 $^3F_3$ + 8.2 $^3H_6$ + 4.8 $^3F_4$
13	16E	7011.5	7012		52.1 $^3F_4$ + 34.6 $^1G_4$ + 4.1 $^3H_6$ + 3.8 $^3F_3$ + 2.7 $^3H_4$ + 2.0 $^3F_2$
13	$9A_1$	7016.8	7012.	4.8	58.3 $^3F_4$ + 34.5 $^1G_4$ + 3.3 $^3H_6$ + 2.0 $^3F_3$ + 1.4 $^3H_4$
14	17E	7121.1	7153		50.2 $^3F_4$ + 34.5 $^1G_4$ + 7.2 $^3F_3$ + 5.3 $^3H_6$ + 1.9 $^3H_4$
14	18E	7156.2	7153.	3.2	63.2 $^3F_4$ + 28.6 $^1G_4$ + 4.6 $^3F_3$ + 1.7 $^3H_6$
	$10A_1$	7183.7			54.5 $^3F_4$ + 36.7 $^1G_4$ + 4.5 $^3H_6$ + 3.2 $^3H_4$
	$8A_2$	7271.3			67.6 $^3F_4$ + 21.7 $^1G_4$ + 8.4 $^3F_3$ + 1.5 $^3H_6$
15	19E	9688.8	9749.[d]	-60.2	56.4 $^1G_4$ + 41.8 $^3F_4$ + 1.0 $^3H_4$
16	$11A_1$	9856.2	9831.[d]	25.2	57.5 $^1G_4$ + 40.6 $^3F_4$ + 1.0 $^3H_4$
17	20E	9921.3	9886.[d]	35.3	59.4 $^1G_4$ + 38.7 $^3F_4$ + 1.2 $^3H_4$
18	$12A_1$	9985.5	9965.[d]	20.5	62.5 $^1G_4$ + 35.5 $^3F_4$ + 1.3 $^3H_4$
19	21E	10358.1	10381.[d]	-22.9	70.1 $^1G_4$ + 27.5 $^3F_4$ + 1.8 $^3H_4$
	$9A_2$	10721.6			74.5 $^1G_4$ + 23.0 $^3F_4$ + 1.9 $^3H_4$
20	22E	16437.5	16462.	-24.5	87.4 $^1D_2$ + 9.4 $^3P_2$ + 2.4 $^3F_2$ + 2.0 $^1D_2$
21	23E	16575.8	16573.	2.8	87.0 $^1D_2$ + 8.6 $^3P_2$ + 2.4 $^3F_2$ + 1.7 $^1I_6$
22	$13A_1$	16870.9	16846.	24.9	84.4 $^1D_2$ + 9.6 $^3P_2$ + 3.9 $^1I_6$ + 2.0 $^3F_2$
23	$14A_1$	20109.9	20109.	0.9	95.8 $^3P_0$ + 2.2 $^3P_2$
24	$10A_2$	20493.3	20515.	-21.7	99.9 $^3P_1$
25	$15A_1$	20728.7	20691.	37.7	99.2 $^1I_6$
26	24E	20763.0	20721.	42.0	84.5 $^3P_1$ + 7.9 $^1I_6$ + 6.5 $^3P_2$
27	25E	20808.1	20820.	-11.9	93.1 $^1I_6$ + 6.1 $^3P_1$
28	26E	20948.0	20929.	19.0	97.8 $^1I_6$ + 1.2 $^3P_2$
29	$16A_1$	21007.7	21044.	-36.3	99.5 $^1I_6$
	$11A_2$	21081.4			99.3 $^1I_6$
30	27E	21188.0	21195.	-7.0	95.7 $^1I_6$ + 3.1 $^3P_2$

Table 1 continued.

Band Number[a]	State	E_{calc} (cm^{-1})	E_{obs} (cm^{-1})	ΔE[b] (cm^{-1})	Eigenvector[c]
31	28E	21559.9	21552.	7.9	$86.2\ ^1I_6 + 11.1\ ^3P_2 + 1.9\ ^3P_1$
32	29E	21684.3	21701.	-16.7	$83.6\ ^3P_2 + 9.6\ ^1D_2 + 6.4\ ^3I_6$
33	$17A_1$	22015.7	22022.	-6.3	$62.3\ ^3P_2 + 32.5\ ^1I_6 + 2.8\ ^3P_0$
34	30E	22164.0	22158.	6.0	$75.6\ ^3P_2 + 9.0\ ^1D_2 + 9.0\ ^1I_6 + 5.9\ ^3P_1$
	$12A_2$	22263.9			$99.7\ ^1I_6$
35	$18A_1$	22709.8	22727.	-17.2	$63.1\ ^1I_6 + 25.2\ ^3P_2 + 10.8\ ^1D_2$
	$19A_2$	45595.0			$98.9\ ^1S_0 + 1.0\ ^3P_0$

[a]Numbers refer to those used in Figures 1-5.

[b]$\Delta E = E_{calc} - E_{obs}$.

[c]Percent of SLJ state. Components are listed which contribute 1.0 percent or greater to the state.

[d]Observed energies from $(MeCp)_3Pr \cdot MeTHF$.

Table 2. Parameter values for Pr^{3+} as the free ion and in various compounds (in cm^{-1})

Parameter	Pr^{3+}(free ion)[a]	$Pr^{3+}/LaCl_3$[b]	$Cp_3Pr \cdot MeTHF$
F^2	71822(35)	68368	66207(62)
F^4	51827(93)	50008	49184(178)
F^6	33890(60)	32743	32543(126)
ζ_{4f}	766(2)	744	742(3)
α	23.9(0.3)	22.9	23.1(0.5)
β	-599(16)	-674	-757(36)
γ	[1400][c]	[1520]	[1534]
M^0	d	1.76[e]	[1.76]
M^2	d	e	[0.99]
M^4	d	e	[0.67]
P^2	166(38)	275	[275]
P^4	d	f	[206]
P^6	d	f	[138]
B_0^2		107	-1200(25)
B_0^4		-342	1301(76)
B_0^6		-677	486(95)
B_3^4		-	290(68)
B_3^6		-	842(77)
B_6^6		466	-2035(59)
F^4/F^2	.72	.73	.74
F^6/F^2	.47	.48	.49
$\zeta_{crys}/\zeta_{free\ ion}$	-	.97	.97

[a]From Ref. 25.
[b]From Ref. 4.
[c]Values in [ ] held fixed in the fitting procedure.
[d]Values for these parameters not given in Ref. 25.
[e]$M^2 = .56\ M^0$; $M^4 = .38\ M^0$
[f]$P^4 = .75\ P^2$, $P^6 = .50\ P^6$

Table 3. Ground State Crystal Field Splittings

	$Cp_3Pr \cdot MeTHF$		$Cp_3Pr \cdot BA$
	Exp.[a] (cm^{-1})	Calc.[a] (cm^{-1})	Exp. (cm^{-1})
$1A_1$	0.0	0.0	0.0
1E	97.	115.7	108.[b]
2E	310.	315.5	330.[b]
$1A_2$	-	340.9	-
3E	756.	715.0	774.
$2A_1$	-	830.7	-

[a]From Table 1.

[b]Used in calculation of the magnetic susceptibility.

Table 4. Ratios of various parameters

Ratio	Pr^{3+}(free ion)[a]	$Pr^{3+}(LaCl_3)$[a]	$Cp_3Pr{\cdot}MeTHF$[a]	U^{4+}(free ion)[b]	$U^{4+}(ThBr_4)$[b]	$U(BD_4)_4$[b]
F^4/F^2	.72	.73	.74	.82	.96	.97
F^6/F^2	.47	.48	.49	.53	.61	.55
F^2_{cry}/F^2_{FI}	–	.96	.92	–	.81	.794
F^4_{cry}/F^4_{FI}	–	.965	.95	–	.95	.936
F^6_{cry}/F^6_{FI}	–	.966	.960	–	.93	.81
ζ_{cry}/ζ_{FI}	–	.97	.97	–	.906	.905

[a]From Table 2.

[b]From Ref. 20.

Figure Captions

Figure 1. The absorption spectrum of $Cp_3Pr \cdot MeTHF$ within the range 2050 - 2500 nm (KBr pellet, temperature: 90 - 100 K).

Figure 2. Absorption spectrum of $Cp_3Pr \cdot MeTHF$ within the range 1370 - 2000 nm. - - - -: at room temperature; •••••: at 90 K; ——— : at 30 K. Bands marked with +, o and ≠ correspond to transitions starting from excited states which have energy separations of 97, 310 and 756 cm^{-1}, respectively, from the crystal field ground state. Bands marked with V are due to vibronic coupling effects. The same notation holds also true for Figures 3 - 5.

Figure 3. Absorption spectrum of $(MeCp)_3 \cdot MeTHF$ within the range 950 - 1070 nm.

Figure 4. Absorption spectrum of $Cp_3Pr \cdot MeTHF$ within the range 580 - 630 nm.

Figure 5. Absorption spectrum of $Cp_3Pr \cdot MeTHF$ within the range 440 - 505 nm.

Figure 6. $1/\chi$ vs. T for $Cp_3Pr \cdot BA$. The experimental data are given as the points. The three curves are drawn (from top to bottom) for k = 0.95, 0.975, and 1.0, respectively.

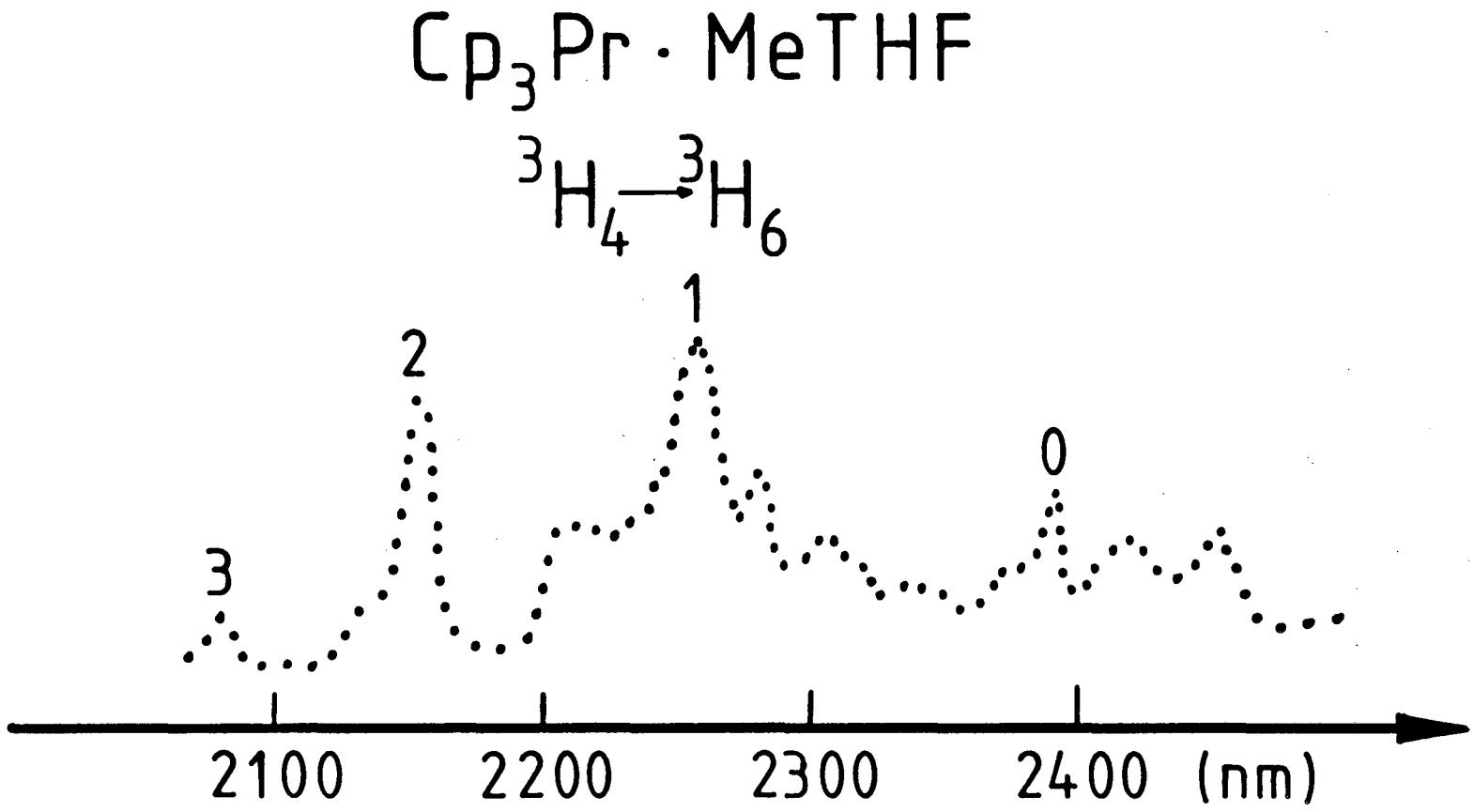

XBL 847-2807

Figure 1

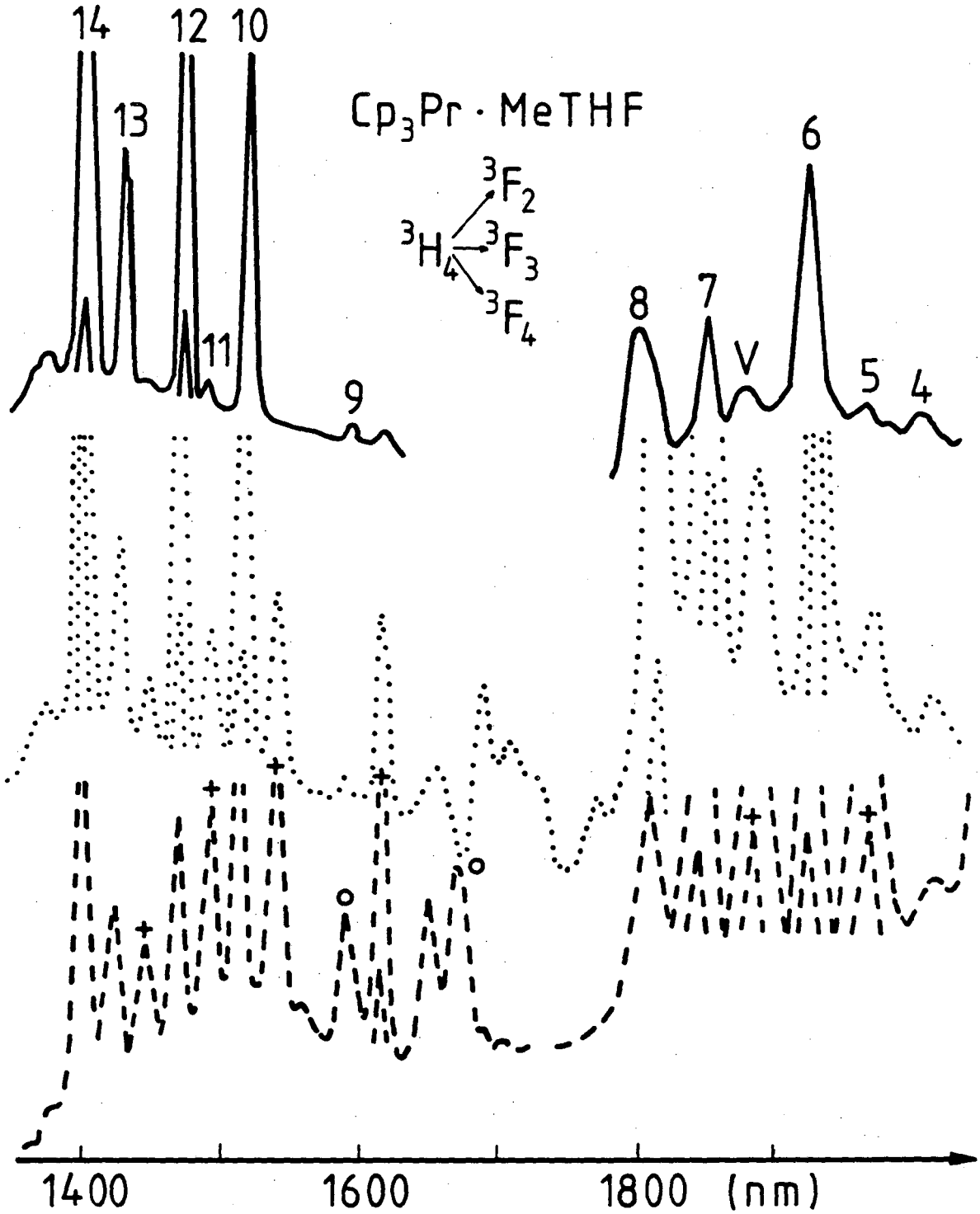

XBL 847-2808

Figure 2

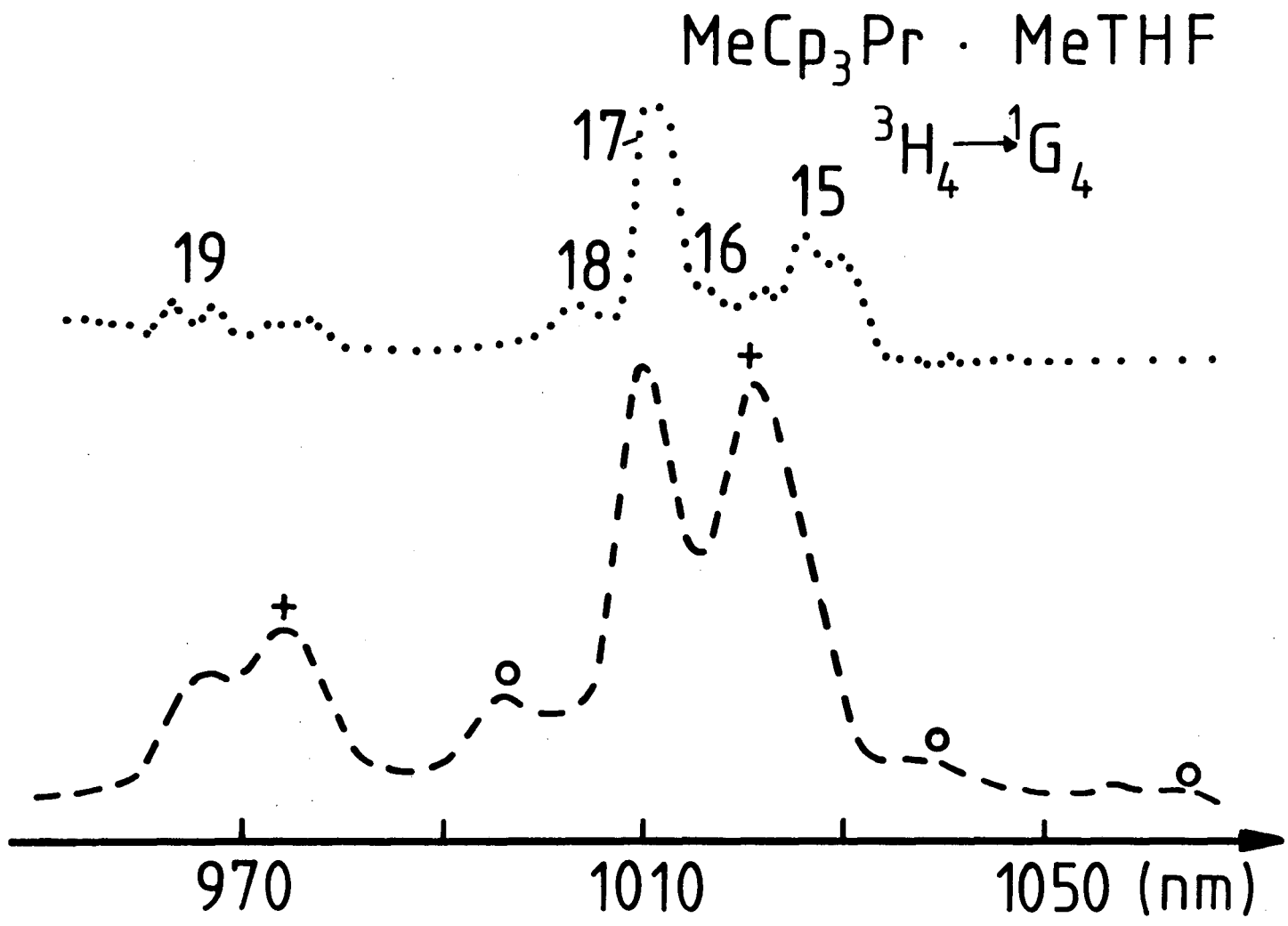

XBL 847-2809

Figure 3

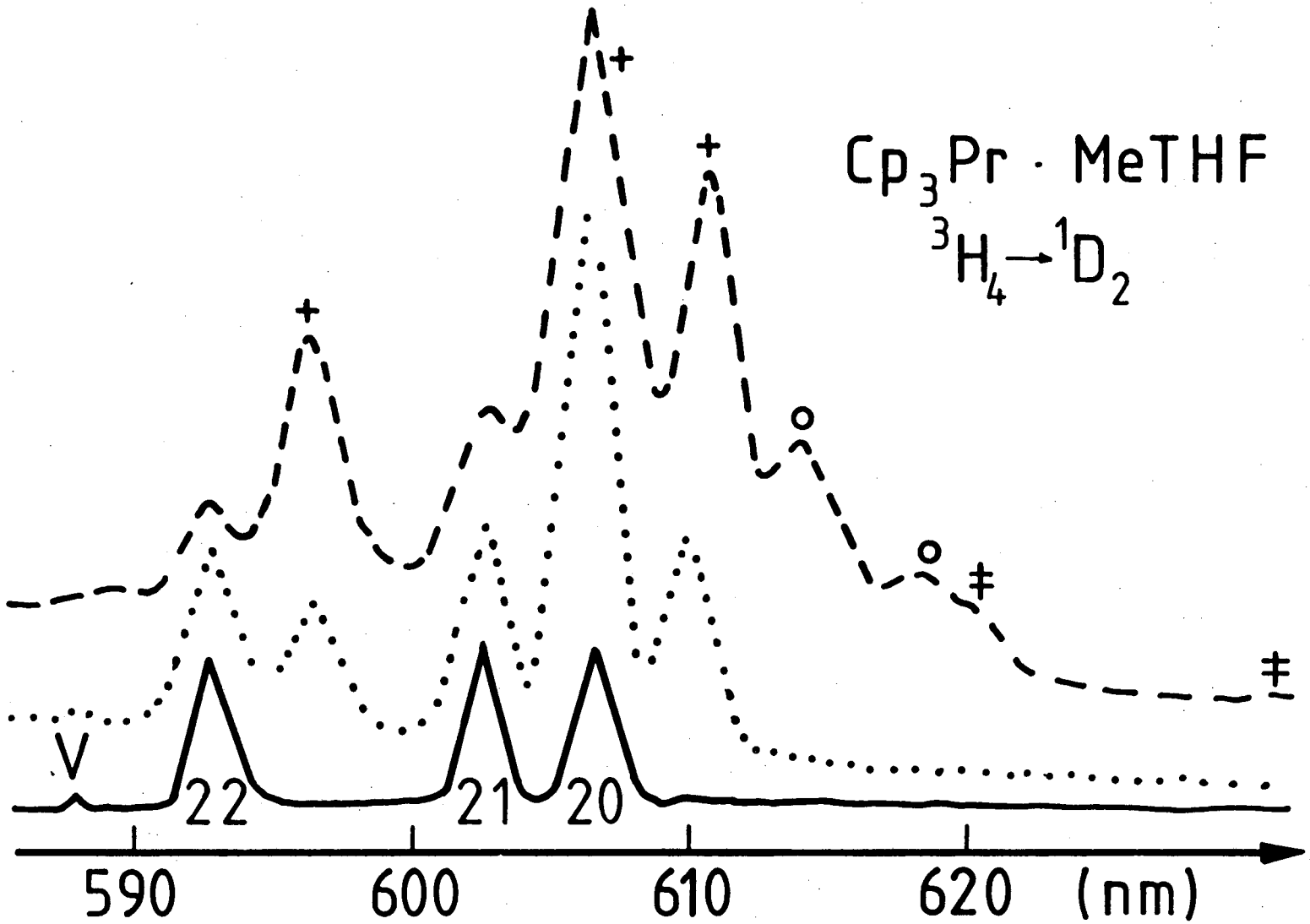

XBL 847-2810

Figure 4

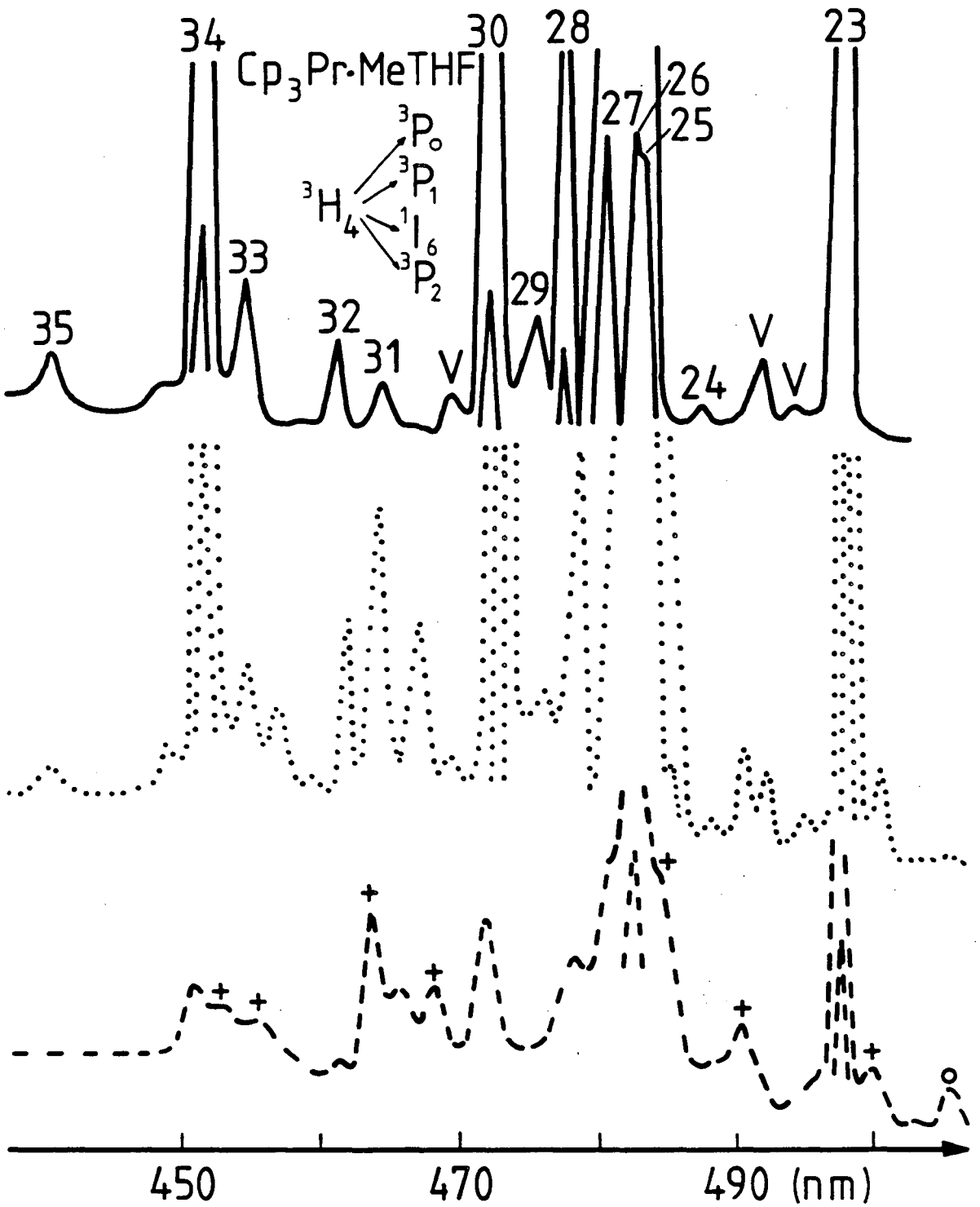

XBL 847-2811

Figure 5

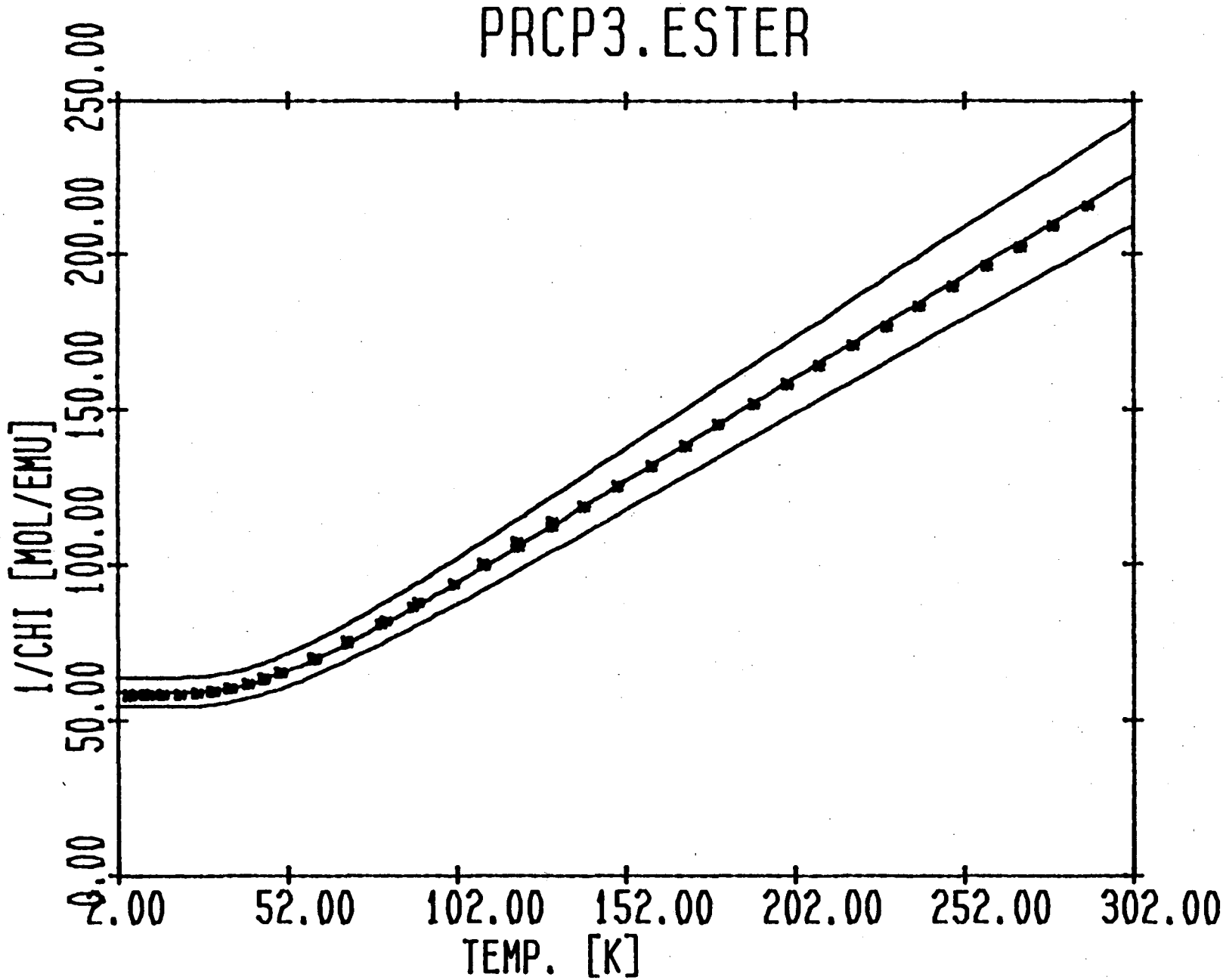
PRCP3.ESTER
1/CHI [MOL/EMU]
0.00
50.00
100.00
150.00
200.00
250.00
2.00
52.00
102.00
152.00
202.00
252.00
302.00
TEMP. [K]

Figure 6

This report was done with support from the Department of Energy. Any conclusions or opinions expressed in this report represent solely those of the author(s) and not necessarily those of The Regents of the University of California, the Lawrence Berkeley Laboratory or the Department of Energy.

Reference to a company or product name does not imply approval or recommendation of the product by the University of California or the U.S. Department of Energy to the exclusion of others that may be suitable.

TECHNICAL INFORMATION DEPARTMENT
LAWRENCE BERKELEY LABORATORY
UNIVERSITY OF CALIFORNIA
BERKELEY, CALIFORNIA 94720